A Multi-Band Transformer for Two Arbitrary Complex Frequency-Dependent Impedances

Ming Chen

Wireless Personal Communications
An International Journal

ISSN 0929-6212

Wireless Pers Commun
DOI 10.1007/s11277-011-0494-1

Springer

Wireless Pers Commun
DOI 10.1007/s11277-011-0494-1

A Multi-Band Transformer for Two Arbitrary Complex Frequency-Dependent Impedances

Ming Chen

Abstract A multi-frequencies transformer for two arbitrary complex frequency-dependent impedances is presented. Design equations of the proposed transformer are derived, and particle swarm algorithm can be used to solve the resulting nonlinear equations. Some numerical examples for two-, three-, and four-section transmission line transformer were presented to verify the validity of the proposed design.

Keywords Complex frequency-dependent impedances · Multi-band · Transmission line transformer · Particle swarm algorithm

1 Introduction

IN modern communication systems, multiband operating components are attractive because of their smaller size and less complexity [1]. In 2002, Chow et al. discovered a two-section transformer that can match at a frequency and its first harmonic [2]. Then Monzon [3] made a comprehensive analysis, derived its closed-form solutions, and extended this construct to match at two arbitrary frequencies for two different real impedances [4]. In [5], complex conjugated loads were discussed at two frequencies. After that, the complex impedance matching problem was solved using two unequal sections [6]. Shortly afterwards, Liu et al. [7] solved dual-frequency transformer for frequency-dependent complex load impedance, and then Wu et al. [8] solved dual-frequency transformer for two arbitrary complex frequency-dependent impedances.

With the development of research on dual-band transmission line transformer (TLT), tri-band [9] and multi-band [10] transformers for real impedances are also investigated. Taking into account of, for general tri- and multi-band microwave circuits (Particularly, active circuits and systems), complex impedances are very common, Chen [11], solved tri-band for

M. Chen (✉)
Institute of Microwave and Optics, Xi'an University of Posts and Telecommunications, Wei Guo Road, Chang'an District, Xi'an 710121, China
e-mail: chenming5628@sina.com

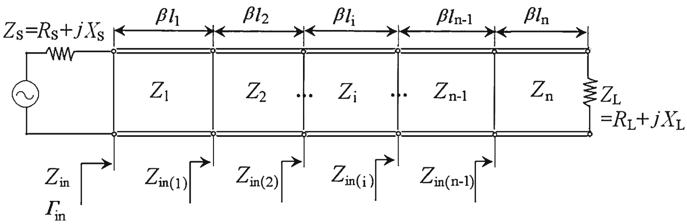

Fig. 1 Multi-section transformer

the complex impedance matching problem, however, these transformers mentioned in [11] are not suitable for a number of matching problems for active devices whose load impedances vary with frequencies, such as low noise amplifiers (LNAs), poweramplifiers (PAs), mixers and microstrip antennas. Therefore, a multi-band transformer for two arbitrary complex frequency-dependent impedances is very useful and imperative in modern communication systems.

How to design the multi-band transformer for two arbitrary complex frequency-dependent impedances is a challenging problem. Although analytical methods based on standard transmission line theory have be successfully used in design the two-band transformer for two arbitrary complex frequency-dependent impedances, however, It is too complex to be difficult to achieve if bands to be matched exceed two, and numerical methods should be used to solve the resulting nonlinear equations. In this paper, a multi-frequency, multi-section TLT for two arbitrary complex frequency-dependent impedances, is investigated and some numerical examples are obtained to verify its validity. Based on an ideal transmission-line model, design equations of the multi-frequency, multi-section TLT for two arbitrary complex frequency-dependent impedances will be given in Sect. 2. The validity of the derived equations are proven by some numerical examples in Sect. 3. Finally, this paper presents conclusions in Sect. 4.

2 Analytical Derivation of Optimization Design Equations of Transformer

A multi-band multi-section lossless transmission lines transformer between two complex impedances ($Z_s = R_s + jX_s$ and $Z_L = R_L + jX_L$) is illustrated in Fig. 1.

The characteristic impedances of the respective transmission-line sections are $Z_1 Z_2, \ldots$, and Z_n. Their respective corresponding physical lengths are $l_1, l_2, \ldots$ and l_n, or their corresponding phase angles $\beta l_{1,} \beta l_2, \ldots$, and βl_n. The driving–point impedances of each section in the n-section TLT (see Fig. 1) are $Z_{\text{in}}, Z_{\text{in}(1)}, Z_{\text{in}(2)}, \ldots, Z_{\text{in}(i)}, \ldots$, and $Z_{\text{in}(n-1)}$, respectively, and they can be expressed by lossless transmission-line circuit equation as follows:

$$Z_{\text{in}} = Z_1 \frac{Z_{\text{in}(1)} + jZ_1 tan\,(\beta l_1)}{Z_1 + jZ_{\text{in}(1)} tan\,(\beta l_1)} \tag{1.1}$$

$$Z_{\text{in}(1)} = Z_2 \frac{Z_{\text{in}(2)} + jZ_2 tan\,(\beta l_2)}{Z_2 + jZ_{\text{in}(2)} tan\,(\beta l_2)} \tag{1.2}$$

$$\cdots$$

$$Z_{\text{in}(i)} = Z_{i+1} \frac{Z_{\text{in}(i+1)} + jZ_{i+1} tan(\beta l_{i+1})}{Z_{i+1} + jZ_{\text{in}(i+1)} tan(\beta l_{i+1})} \tag{1. i+1}$$

$$\cdots$$

$$Z_{\text{in}(n-1)} = Z_n \frac{Z_L + jZ_n tan(\beta l_n)}{Z_n + jZ_L tan(\beta l_n)} \tag{1.n}$$

Equation (1.1)–(1.n) give the dependence of $Z_{\text{in}}, Z_{\text{in}(1)}, Z_{\text{in}(2)}, \ldots,$ and $Z_{\text{in}(n-1)}$ on frequency f. The frequencies to be matched can be chosen so that $f_2 = u_1 f_1$, $f_3 = u_2 f_1, \ldots, f_n = u_{n-1} f_1$, where $u_1, u_2, \ldots,$ and u_{n-1} are positive numbers. For perfect matching at frequencies $f_1, f_2, \ldots, f_n$, simultaneously, let $Z_{\text{in}}(f_i)|_{i=1,2,\ldots,n} = Z_S^*(f_i)|_{i=1,2,\ldots,n}$, where $Z_S^*(f_i) = conj\,[Z_S(f_i)]$, the $Z_{\text{in}}(f_1), Z_{\text{in}}(f_2), \ldots,$ and $Z_{\text{in}}(f_n)$ are the input impedance at frequencies $f_1, f_2, \ldots,$ and f_n, respectively, and their related reflection coefficients are $\Gamma_1(f_1), \Gamma_2(f_2), \ldots,$ and $\Gamma_n(f_n)$, which can be concisely expressed as [12]

$$\Gamma_i(f_i) = \frac{Z_{\text{in}}(f_i) - Z_S^*(f_i)}{Z_{\text{in}}(f_i) + Z_S(f_i)} \quad (i = 1, 2, \ldots, n) \tag{2}$$

The goal of the design is to find the characteristic impedances $Z_1, Z_2, \ldots, Z_n$, and their corresponding physical lengths $l_1, l_2, \ldots, l_n$, or corresponding phase angles $\beta l_1, \beta l_2, \ldots,$ and βl_n. For compact design, constraint conditions is as follows

$$Z_1 > 0, Z_2 > 0, \ldots, Z_n > 0 \tag{3.1}$$
$$0 < \beta_1 l_m|_{m=1,2,\ldots,n} < \pi/2 \tag{3.2}$$

where β_1 is the phase constant at f_1. Further, based on the method of least squares (MLS), the design of the multi-band transformer for two arbitrary complex frequency-dependent impedances can be summarized following optimization equations

$$F = \sum_{i=1}^{n} (|\Gamma_i(f_i)| - \varepsilon_i(f_i))^2 \tag{4.1}$$

with Eqs. (3.1) and (3.2), where ε_i is optimization target, it can be chosen to satisfy the following equation for required reflection coefficient in dB at matched frequency,

$$20\lg(\varepsilon(f_i))|_{i=1,2,\ldots,n} \leq -23\,\text{dB} \tag{4.2}$$

For example, for tri-frequency three-section TLT, we have

$$F = \sum_{i=1}^{3} (|\Gamma_i(f_i)| - \varepsilon_i(f_i))^2 \tag{5.1}$$
$$Z_1 > 0, \quad Z_2 > 0, \quad Z3 > 0 \tag{5.2}$$
$$0 < \beta_1 l_m|_{m=1,2,3} < \pi/2 \tag{5.3}$$

Optimization equations above mentioned can be solved using particle swarm algorithm (PSA) [13,14]. Let X denotes position matrix, V the velocity matrix, P the personal matrix, G the global best position. To move each particle closer to both its personal best and global best position, the velocity matrix and the position matrix are updated according to following Eqs. (6) and (8), respectively

$$V_{mn}^i = wV_{mn}^{i-1} + c_1 \times rand_1 \times \left(P_{mn}^i - X_{mn}^{i-1}\right) \tag{6}$$
$$+ c_2 \times rand_2 \times \left(G_n^i - X_{mn}^{i-1}\right) \tag{7}$$
$$X^i = X^{i-1} + V^i \tag{8}$$

where the superscripts i and $i-1$ refer to the time index of the current and the previous iterations, $rand_1$ and $rand_2$ are uniformly distributed random numbers in the interval [0,1]. The parameters c_1 and c_2, called cognition and social acceleration, specify the relative weight of the personal best position versus the global best position. The parameter w, called the "inertial weight", is a number in the range [0, 1], and it specifies the weight by which the particle's current velocity depends on its previous velocity and the distance between the particle's location and its personal best and global best positions [14]. In order to find the characteristic impedances $Z_1, Z_2, \ldots$, and Z_n, and their corresponding physical lengths $l_1, l_2, \ldots$, and l_n, let Eq. (4.1) with Eqs. (4.2), (3.1) and (3.2) act as the fitness function. The following points are the steps of the MLS with the PSO algorithm:

1. Determine specifications (i.e., the matching frequencies $f_1, f_2, \ldots, f_n$, the number of this section of transformer, the source equivalent impedances $Z_{si}(f_i) = R_{si}(f_i) + jX_{si}(f_i)|_{i=1,2,\ldots,n}$, and the load impedances $Z_{Li}(f_i) = R_{Li}(f_i) + jX_{Li}(f_i)|_{i=1,2,\ldots,n}$.
2. Initialize the position and velocity of the particles randomly in the problem space.
3. Use the current position vector of each particle to evaluate the fitness value using (4.1) with Eq. (4.2), (3.1) and (3.2).
4. Compare the particle's fitness value with the particle's pbest. If the current value is better (here better numerically means smaller) than pbest, then replace pbest by the current value, and the particle's position vector by the current position vector.
5. Compare the current fitness value with the global previous best. If the current value is better than gbest, then set gbest and G to the current value and position, respectively
6. Update the particle's velocity and position according to (7).
7. Repeat starting from step (2) until a stopping criterion is met: a good fitness value or a maximum number of iterations.

A Matlab programming code was developed for the solution process.

3 Numerical Examples

In this section, two complex frequency-dependent impedances are considered, and three kinds of transformers (dual-band, tri-band, and four-band) with 9 types illustrated in following A, B and C of this section respectively, are presented to verify the proposed design method. The real and imaginary parts of source and load equivalent impedances are given in Fig. 2.

3.1 Numerical Examples for Dual-Band Two-Section Transformer

The goal is to match these two impedances at two different frequencies. Here, three situations are taken into account as follows:

First, given

$$Z_{S1} = 33.8 + j25.9 \text{ at } f_1 = 1\,\text{GHz}$$
$$Z_{S2} = 38.7301 + j23.0121 \text{ at } f_2 = 2\,\text{GHz}$$

while

$$Z_{L1} = 140 + j60 \text{ at } f_1 = 1\,\text{GHz}$$
$$Z_{L2} = 133.1821 + j53.1821 \text{ at } f_2 = 2\,\text{GHz}$$

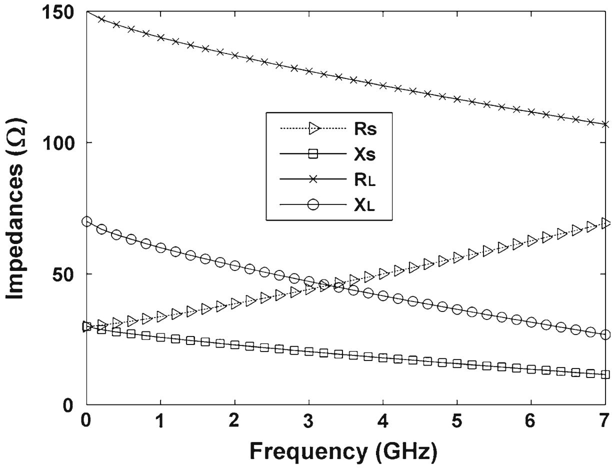

Fig. 2 Source and load impedances varying with the operating frequency

Table 1 Design parameters of the dual-band transformer

Type	$Z_1(\Omega)$	$Z_2(\Omega)$	l_1/λ_1	l_2/λ_1
1	58.6413	111.1108	0.1101	0.2081
2	57.9304	111.3959	0.1091	0.2085
3	71.9493	94.2487	0.1179	0.1598

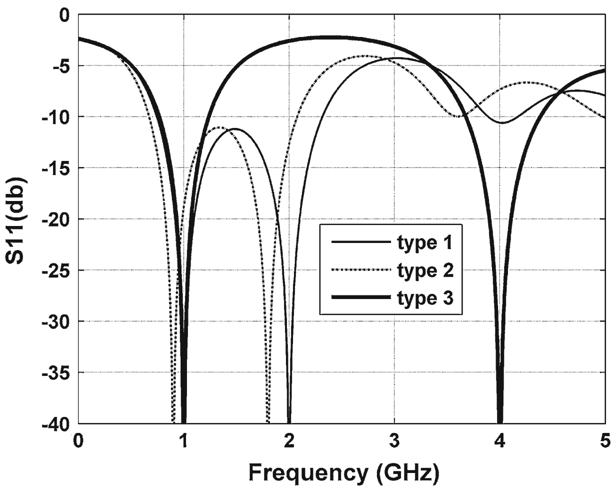

Fig. 3 Simulated results of dB S11 versus frequency

simulation results of the TLT obtained from (4.1) with (4.2), (3.1) and (3.2) are presented in type 1 of Table 1, and the corresponding dependence of reflection coefficient in dB on frequency is presented in Fig. 3.

Second, given

$$Z_{S1} = 33.3487 + j26.2192 \text{ at } f_1 = 0.9\,\text{GHz}$$
$$Z_{S2} = 37.6933 + j23.5561 \text{ at } f_2 = 1.8\,\text{GHz}$$

while

$$Z_{L1} = 140.7598 + j60.7598 \text{ at } f_1 = 0.9\,\text{GHz}$$
$$Z_{L2} = 134.4599 + j54.4599 \text{ at } f_2 = 1.8\,\text{GHz}$$

simulation results of the TLT obtained from (4.1) with (4.2), (3.1) and (3.2) are presented in type 2 of Table 1, and the corresponding dependence of reflection coefficient in dB on frequency is presented in Fig. 3.

Third, given

$$Z_{S1} = 40.8652 + j21.96 \text{ at } f_1 = 2.4\,\text{GHz}$$
$$Z_{S2} = 61.3254 + j14.1497 \text{ at } f_2 = 5.8\,\text{GHz}$$

while

$$Z_{L1} = 130.7177 + j50.7177 \text{at} f_1 = 2.4\,\text{GHz}$$
$$Z_{L2} = 112.6259 + j32.6259 \text{ at } f_2 = 5.8\,\text{GHz}$$

simulation results of the TLT obtained from (4.1) with (4.2), (3.1) and (3.2) are presented in type 3 of Table 1, and the corresponding dependence of reflection coefficient in dB on frequency is presented in Fig. 3.

From the final matching responses in Fig. 3, it can be observed clearly that the two complex frequency-dependent impedances are matched at two different frequencies, simultaneously. Note that the matching bandwidth at each frequency depends on the values of matched impedances and the frequency ratio.

3.2 Numerical Examples for Tri-Band Three-Section Transformer

The goal is to match these three impedances at three different frequencies. Here, three situations are taken into account as follows:

First, given

$$Z_{S1} = 33.8 + j25.9 \text{ at } f_1 = 1\,\text{GHz}$$
$$Z_{S2} = 38.7301 + j23.0121 \text{ at } f_2 = 2\,\text{GHz}$$
$$Z_{S3} = 44.2013 + j20.4545 \text{ at } f_3 = 3\,\text{GHz}$$

while

$$Z_{L1} = 140 + j60 \text{ at } 1\, f_1 = \text{GHz}$$
$$Z_{L2} = 133.1821 + j53.1821 \text{ at } f_2 = 2\,\text{GHz}$$
$$Z_{L3} = 127.2049 + j47.2049 \text{ at} f_3 = 3\,\text{GHz}$$

simulation results of the TLT obtained from (4.1) with (4.2), (3.1) and (3.2) are presented in type 4 of Table 2, and the corresponding dependence of reflection coefficient in dB on frequency is presented in Fig. 4.

Table 2 Design parameters of the three-band transformer

Type	$Z_1(\Omega)$	$Z_2(\Omega)$	$Z_3(\Omega)$	l_1/λ_1	l_2/λ_1	l_3/λ_1
4	54.9353	98.9762	140.0000	0.0796	0.1176	0.1812
5	46.3567	94.6969	140.7598	0.0660	0.1378	0.1832
6	59.1717	84.5942	106.7034	0.0751	0.0874	0.1335

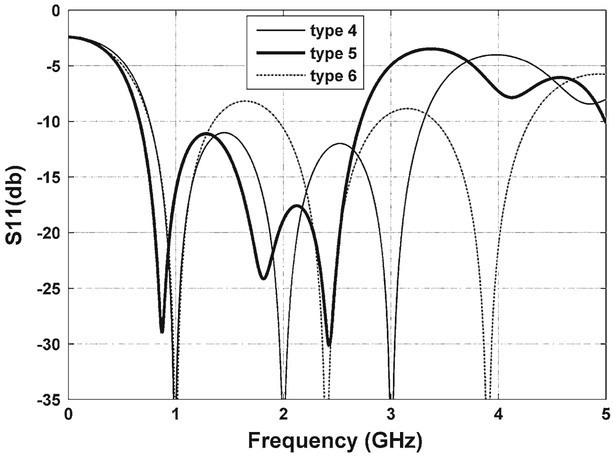

Fig. 4 Simulated results of dB S11 versus frequency

Second, given

$$\begin{aligned} Z_{S1} &= 33.3487 + j26.2192 \text{ at } f_1 = 0.9\,\text{GHz} \\ Z_{S2} &= 37.6933 + j23.5561 \text{ at } f_2 = 1.8\,\text{GHz} \\ Z_{S3} &= 40.8652 + j21.9600 \text{ at } f_3 = 2.4\,\text{GHz} \end{aligned}$$

while

$$\begin{aligned} Z_{L1} &= 140.7598 + j60.7598 \text{ at } f_1 = 0.9\,\text{GHz} \\ Z_{L2} &= 134.4599 + j54.4599 \text{ at } f_2 = 1.8\,\text{GHz} \\ Z_{L3} &= 130.7177 + j50.7177 \text{ at } f_3 = 2.4\,\text{GHz} \end{aligned}$$

simulation results of the TLT obtained from (4.1) with (4.2), (3.1) and (3.2) are presented in type 5 of Table 2, and the corresponding dependence of reflection coefficient in dB on frequency is presented in Fig. 4.

Third, given

$$\begin{aligned} Z_{S1} &= 33.8 + j25.9 \text{ at } f_1 = 1\,\text{GHz} \\ Z_{S2} &= 40.8652 + j21.9600 \text{ at } f_2 = 2.4\,\text{GHz} \\ Z_{S3} &= 49.4563 + j18.3198 \text{ at } f_3 = 3.9\,\text{GHz} \end{aligned}$$

Table 3 Design parameters of the four-band transformer

Type	$Z_1(\Omega)$	$Z_2(\Omega)$	$Z_3(\Omega)$	$Z_4(\Omega)$	l_1/λ_1	l_2/λ_1	l_3/λ_1	l_4/λ_1
7	38.9066	54.0335	72.0487	132.0129	0.1301	0.2028	0.2039	0.2413
8	37.3873	61.7762	69.3294	126.1685	0.2439	0.1217	0.1856	0.1195
9	49.4352	96.4440	138.3071	89.4886	0.0741	0.1303	0.1331	0.0255

while

$$
\begin{aligned}
Z_{L1} &= 140 + j60 \text{ at } f_1 = 1\,\text{GHz} \\
Z_{L2} &= 130.7177 + j50.7177 \text{ at } f_2 = 2.4\,\text{GHz} \\
Z_{L3} &= 122.2477 + j42.2477 \text{ at } f_3 = 3.9\,\text{GHz}
\end{aligned}
$$

simulation results of the TLT obtained from (4.1) with (4.2), (3.1) and (3.2) are presented in type 6 of Table 2. The corresponding dependence of reflection coefficient in dB on frequency is presented in Fig. 4.

From the final matching responses in Fig. 3, it can be observed clearly that the two complex frequency-dependent impedances are matched at three different frequencies, simultaneously. Note that the matching bandwidth at each frequency depends on the values of matched impedances and the frequency ratio.

3.3 Numerical Examples for Quad-Band 4-Section Transformer

The goal is to match these four impedances at four different frequencies. Here, three situations are taken into account as follows:

First, given

$$
\begin{aligned}
Z_{S1} &= 33.8 + j25.9 \text{ at } f_1 = 1\,\text{GHz} \\
Z_{S2} &= 38.7301 + j23.0121 \text{ at } f_2 = 2\,\text{GHz} \\
Z_{S3} &= 44.2013 + j20.4545 \text{ at } f_3 = 3\,\text{GHz} \\
Z_{S4} &= 50.0565 + j18.0901 \text{ at } f_4 = 4\,\text{GHz}
\end{aligned}
$$

while

$$
\begin{aligned}
Z_{L1} &= 140 + j60 \text{ at } f_1 = 1\,\text{GHz} \\
Z_{L2} &= 133.1821 + j53.1821 \text{ at } f_2 = 2\,\text{GHz}, \\
Z_{L3} &= 127.2049 + j47.2049 \text{ at } f_3 = 3\,\text{GHz} \\
Z_{L4} &= 121.7157 + j41.7157 \text{ at } f_4 = 4\,\text{GHz}
\end{aligned}
$$

simulation results of the TLT obtained from (4.1) with (4.2), (3.1) and (3.2) are presented in type 7 of Table 3. The corresponding dependence of reflection coefficient in dB on frequency is presented in Fig. 5.

Second, given

$$
\begin{aligned}
Z_{S1} &= 33.3487 + j26.2192 \text{ at } f_1 = 0.9\,\text{GHz} \\
Z_{S2} &= 37.6933 + j23. \text{ at } f_2 = 1.8\,\text{GHz} \\
Z_{S3} &= 40.8652 + j21.9600 \text{ at } f_3 = 2.4\,\text{GHz} \\
Z_{S4} &= 47.6745 + j19.0173 \text{ at } f_4 = 3.6\,\text{GHz}
\end{aligned}
$$

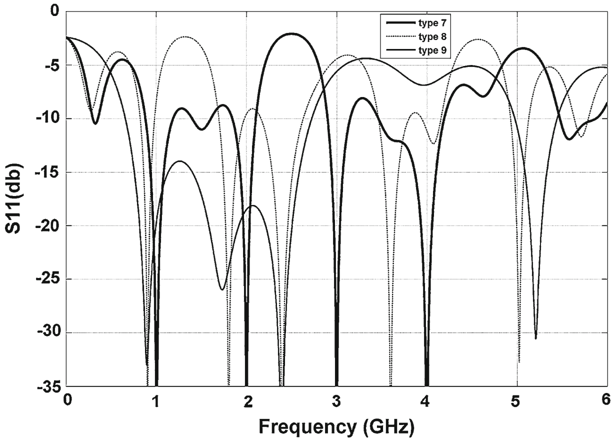

Fig. 5 Simulated results of dB S11 versus frequency

while

$$\begin{aligned} Z_{L1} &= 140.7598 + j60.7598 \text{ at } f_1 = 0.9\,\text{GHz} \\ Z_{L2} &= 134.4599 + j54.4599 \text{ at } f_2 = 1.8\,\text{GHz} \\ Z_{L3} &= 130.7177 + j50.7177 \text{ at } f_3 = 2.4\,\text{GHz} \\ Z_{L4} &= 123.8647 + j43.8647 \text{ at } f_4 = 3.6\,\text{GHz} \end{aligned}$$

simulation results of the TLT obtained from (4.1) with (4.2), (3.1) and (3.2) are presented in type 8 of Table 3. The corresponding dependence of reflection coefficient in dB on frequency is presented in Fig. 5.

Third, given

$$\begin{aligned} Z_{S1} &= 33.3487 + j26.2192 \text{ at } f_1 = 0.9\,\text{GHz} \\ Z_{S2} &= 37.6933 + j23.5561 \text{ at } f_2 = 1.8\,\text{GHz} \\ Z_{S3} &= 40.8652 + j21.96 \text{ at } f_3 = 2.4\,\text{GHz} \\ Z_{S4} &= 57.4782 + j15.4268 \text{ at } f_4 = 5.2\,\text{GHz} \end{aligned}$$

while

$$\begin{aligned} Z_{L1} &= 140.7598 + j60.7598 \text{ at } f_1 = 0.9\,\text{GHz} \\ Z_{L2} &= 134.4599 + j54.4599 \text{ at } f_2 = 1.8\,\text{GHz} \\ Z_{L3} &= 130.7177 + j50.7177 \text{ at } f_3 = 2.4\,\text{GHz} \\ Z_{L4} &= 115.5648 + j35.5648 \text{ at } f_4 = 5.2\,\text{GHz} \end{aligned}$$

simulation results of the TLT obtained from (4.1) with (4.2), (3.1) and (3.2) are presented in type 9 of Table 3. The corresponding dependence of reflection coefficient in dB on frequency is presented in Fig. 5.

From the final matching responses in Fig. 5, it can be observed clearly that the two complex frequency-dependent impedances are matched at four different frequencies, simultaneously. Note that the matching bandwidth at each frequency depends on the values of matched impedances and the frequency ratio.

4 Conclusion

A generalized multi-band multi-section transformer for two arbitrary complex frequency-dependent impedances is presented in this letter. Some simple design equations of the proposed transformer are derived, and algorithm for proposed design equations is discussed. Numerical examples verify the proposed structure and the design method. It is believed that this generalized transformer can be used widely in multi-band or wide-band microwave circuits and systems as an internal matching structure.

Acknowledgments This work is supported by National Natural Science Foundation of China (Project Grant no. 61040064).

References

1. Webb, W. (2003). *The complete wireless communications professional: A guide for engineers and managers*. Boston, MA: Artech House.
2. Chow, Y. L., & Wan, K. L. (2002). A transformer of one-third wavelength in two sections-for a frequency and its first harmonic. *IEEE Microwave and Wireless Components Letters, 12*(1), 22–23.
3. Monzon, C. (2002). Analytical derivation of a two-section impedance transformer for a frequency and it first harmonic. *IEEE Microwave and Wireless Components Letters, 12*(10), 381–382.
4. Monzon, C. (2003). A small dual-frequency transformer in two sections. *IEEE Transactions on Microwave Theory and Techniques, 51*(4), 1157–1161.
5. Colantonio, P., Giannini, F., Scucchia, L. (2004). A newapproach to design matching networks with distributed elements. In *Proceedings of the MIKON'04* (Vol. 3, pp. 811–814).
6. Wu, Y., Liu, Y., & Li, S. (2009). A dual-frequency transformer for complex impedances with two unequal sections. *IEEE Microwave and Wireless Components Letters, 19*(2), 77–79.
7. Liu, X., Liu, Y. A., Li, S. L., Wu, F., & Wu, Y. (2009). A three-section dual-band transformer for frequency-dependent complex load impedance. *IEEE Microwave and Wireless Components Letters, 19*(10), 611–613.
8. Wu, Y., Liu, Y. A., Li, S. L., Yu, C. P., & Liu, X. (2009). A generalized dual-frequency transformer for two arbitrary complex frequency-dependent impedances. *IEEE Microwave and Wireless Components Letters, 19*(12), 611–613.
9. Chongcheawchamnan, M., Patisang, S., Srisathit, S., Phromloungsri, R., & Bunnjaweht, S. (2005). Analysis and design of a three-section transmission-line transformer. *IEEE Transactions on Microwave Theory and Techniques, 53*(7), 2458–2462.
10. Chen, M. (2008). Novel design method of a multi-section transmission-line transformer using genetic algorithm techniques. In *11th international conference on electrical machines and systems, ICEMS 2008*, Wuhan, China, Oct. 17–20.
11. Chen, M. (2011). A three-frequency transformer for complex impedances with three-section. *Chinese Journal of Electronics, 20*, 343–346.
12. Kurokawa, K. (1965). Power waves and the scattering matrix. *IEEE Transactions on Microwave Theory and Techniques, MTT-13*(3), 194–202.
13. Kennedy, J., Eberhart, R. (1995). Particle swarm optimization. In *Proceedings IEEE international conference on neural networks* (Vol. IV, pp 1942–1948). Perth, Australia, November/December 1995.
14. Eberhart, R. C., Shi, Y. (2001). Particle swarm optimization: Developments, applications and resources. In *Proceedings congress on evolutionary computation* (pp 81–86), Seoul, Korea.

Author Biography

Ming Chen received the B.Sc. degree in radio electronics from the Wuhan University, Wuhan, China, in 1982. the Ph.D. degree in electronic science and technology from Xi'an Jiaotong University, Xi'an, China in 2003. He is currently a Director of the Research Center of Microwave & Optics and Professor with the Department of Electromagnetic-Wave Applications and Wireless Technology, Xi'an University of Posts & Telecommunications, Xi'an, China. His research and teaching interests include RF/microwave circuits and integrated optics.